Journal of the Indian Institute of Science, Bangalore 560 012, India

[Section A : Engineering and Technology]

Volume 62 *March* 1980 *Number* 3

CONTENTS

Published by T. K. S. Iyengar, Executive Editor, Journal of the Indian Institute of Science Bangalore 560 012 and Printed at the Bangalore Press, Bangalore 560 018

J. Indian Inst. Sci. 62 (A), Mar 1980, Pp. 57–69

Effect of wave parameters on flood wave subsidence

M. S. MOHAN KUMAR AND K. SRIDHARAN
Department of Civil Engineering, Indian Institute of Science, Bangalore 560 012.

Received on March 5, 1980.

Abstract

A detailed analysis on the propagation of a sinusoidal flood wave in a wide prismatic open channel has been made by numerically integrating the governing nondimensional equations of unsteady flow in an open channel. Emphasis has been laid on the effect of wave parameters on the propagation of the sinusoidal wave. Results show that the amount of subsidence is more in the case of small wave amplitude and wave duration cases. Further, wave duration has been noticed to have a relatively higher influence on subsidence than wave amplitude. The speed at which the peak of the wave moves is observed to be a function of only the wave amplitude.

Key words : Floods, hydraulics, open channel flows, wave subsidence.

1. Introduction

A parametric study on the effect of different governing parameters on the propagation of a flood wave is scarce. Importance has been generally given only to the methods of solution of the flood wave problem[1]. The effects of bed slope, roughness and wave amplitude on flood wave subsidence was studied by Mozayeny and Song[2] for a specific case. They have studied the effect of wave amplitude and bed slope on the propagation of a sinusoidal flood wave in a long prismatic open channel of 0·3 m (1 ft) width in which the initial flow was uniform with a depth of 0·09 m (0·3 ft). The wave duration of the sinusoidal wave was 30 secs with wave amplitude varying from 0·06 cm (0·002 ft) to 0·6 cm (0·02 ft). While these results give an indication of the damping of a flood wave in prismatic channels, the studies are confined to a specific channel and specific initial flow which makes it impossible to interpret the results more generally. Further the wave amplitudes considered by them are very small relative to the initial uniform flow depth. By making a nondimensional parametric study, a generalised picture of damping of a flood wave may be obtained. A somewhat similar study has been reported by Chin-lien Yen[3] in a situation where the storage effect is the dominant factor. This paper presents a parametric study of subsidence where storage is not

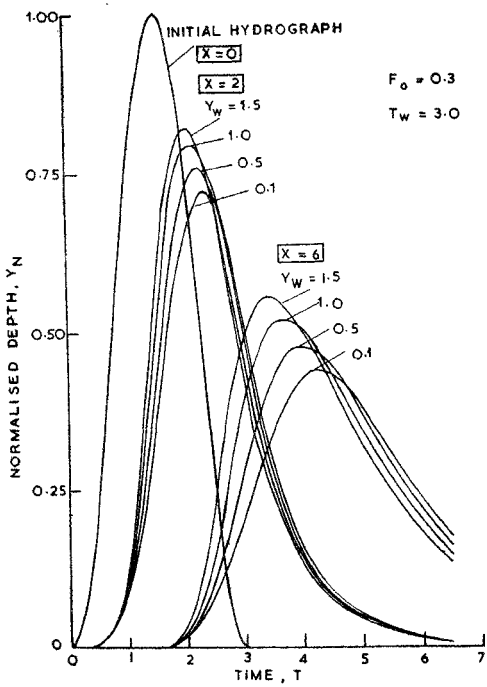

FIG. 1. Effect of wave amplitude on stage hydrograph.

the dominant factor as in a wide prismatic channel. Attention is focussed on the effect of wave parameters on subsidence. Effect of wave parameters, namely, wave amplitude and wave duration, on the propagation of a sinusoidal flood wave in a wide channel in which the initial flow is uniform has been studied.

2. Governing equations and formulation of the problem

The governing equations of unsteady flow in wide open channels are given by

$$v\frac{\partial y}{\partial x} + y\frac{\partial v}{\partial x} + \frac{\partial y}{\partial t} = 0 \tag{1}$$

$$v\frac{\partial v}{\partial x} + g\frac{\partial y}{\partial x} + \frac{\partial v}{\partial t} = g(S_0 - S_f) \tag{2}$$

where x is the distance along the channel; t is the time; y is the depth of flow; v is the velocity of flow; g is the acceleration due to gravity; S_0 is the bed slope and S_f is the friction slope.

The governing equations of the flow are nondimensionalised to enable a generalised parametric study. The nondimensional depth, velocity and time are defined as,

$$Y = \frac{y}{y_0}; \quad V = \frac{v}{v_0}$$

$$X = \frac{x}{l_0} = \frac{xS_0}{y_0}; \quad T = \frac{t}{t_0} = \frac{tv_0}{l_0} \tag{3}$$

where y_0 is the initial uniform flow depth and v_0 is the uniform velocity. Using eqns. (3) and Manning's formula, eqns. (1) and (2) become,

$$V\frac{\partial Y}{\partial X} + Y\frac{\partial V}{\partial X} + \frac{\partial Y}{\partial T} = 0 \tag{4}$$

$$\frac{\partial Y}{\partial X} + F_0^2 V\frac{\partial V}{\partial X} + F_0^2\frac{\partial V}{\partial T} = 1 - V^2 Y^{-4/3} \tag{5}$$

where

$$F_0 = \frac{v_0}{\sqrt{gy_0}} \tag{6}$$

is the initial uniform flow Froude number.

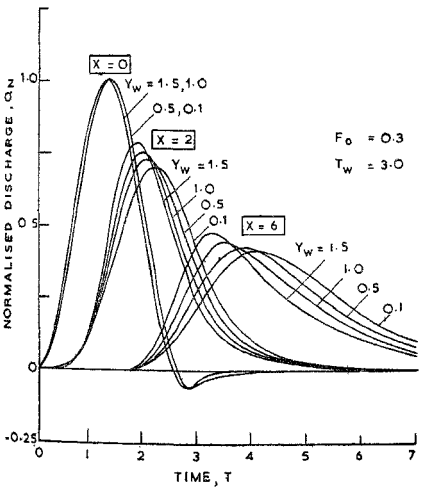

FIG. 2. Effect of wave amplitude on discharge hydrograph.

A sinusoidal wave is now introduced at the left boundary and takes the nondimensional form

$$Y = 1 + \frac{Y_w}{2}\left[1 - \cos\left(\frac{2\pi T}{T_w}\right)\right]; \quad 0 \leqslant T \leqslant T_w$$

$$Y = 1; \quad T > T_w \tag{7}$$

where

$$Y_w = \frac{y_w}{y_0}; \quad T_w = \frac{t_w}{t_0} \tag{8}$$

are the nondimensional wave amplitude and wave duration respectively. A uniform flow boundary condition is imposed on the right boundary, that is, the channel is considered long.

The problem of subsidence of sinusoidal wave is governed by eqns. (4), (5) and (7). The parameters governing this problem are, initial uniform flow Froude number F_0, wave amplitude Y_w and wave duration T_w. In the present study, the effects of variations in wave amplitude and wave duration on subsidence is studied. The nondimensional wave amplitude Y_w is varied from 0·1 to 1·5 and the nondimensional wave duration is varied from 0·5 to 3·0. The third parameter of the problem, namely, initial uniform flow Froude number F_0 is chosen at 0·3.

The problem is solved numerically by using the direct explicit finite difference method on a staggered rectangular grid[4].

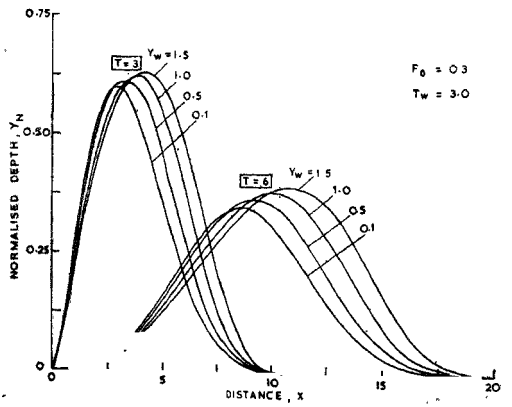

FIG. 3. Effect of wave amplitude on wave front.

3. Effect of wave amplitude

3.1. *Modification of hydrographs*

3.1.1. *Stage hydrograph*

Superimposed normalised hydrographs for different wave amplitudes are presented in Fig. 1. for the case with $F_0 = 0{\cdot}3$ and $T_w = 3{\cdot}0$. The nondimensional normalised depth Y_N is defined as

$$Y_N = \frac{Y - 1}{Y_w} . \tag{9}$$

This normalisation reduces the hydrograph at $X = 0$ to the same shape for all Y_w values, enabling a study of the relative subsidence of the wave form for diffrent wave amplitudes. It is clear from the figure that initial wave disturbance is felt practically at the same time at a given location for all Y_w values confirming that the speed of the propagation of the initial disturbance is dependent on the initial flow Froude number only. However, it is seen that the speed of propagation of the wave peak is clearly dependent on the wave amplitude. The wave peak arrives earlier at a particular section for higher wave amplitudes confirming that the higher amplitude wave travels faster (celerity of the gravity wave is directly proportional to the square root of depth). The difference in the time of arrival of the peak for different wave amplitudes is seen conspicuously in the hydrograph at $X = 6$.

The wave amplitude Y_w has a noticeable effect on the relative damping. The damping is relatively less for higher wave amplitudes and hence a linearising assumption (such as used in the unit hydrograph theory) does not strictly hold good. This was also indicated by the results of Mozayeny and Song[2].

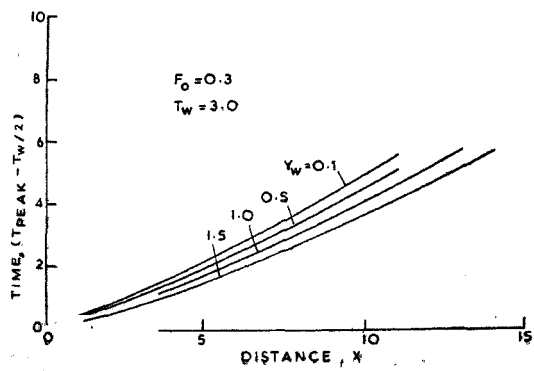

FIG. 4. Speed of travel of wave peak for different wave amplitudes.

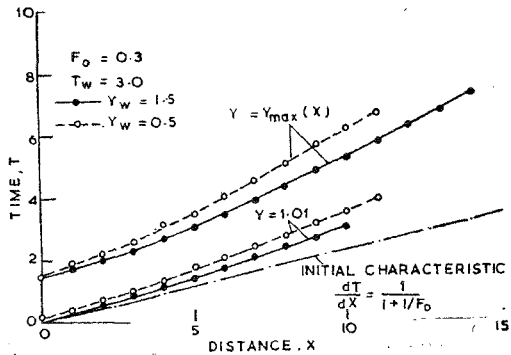

FIG. 5. Path of wave in XT plane.

3.1.2. *Discharge hydrograph*

Figure 2 presents a superposed picture of the discharge hydrographs for different wave amplitudes. Q_N, the normalised discharge rise, which is analogous to the normalised depth rise Y_N, is defined as

$$Q_N = \frac{Q(X) - 1}{Q(0) - 1}. \tag{10}$$

In Fig. 2, Q_N is plotted against time T at $X = 0$, 2 and 6 for different wave amplitudes. The normalised hydrograph at $X = 0$ is practically the same for all Y_N values and the tail end of the hydrograph dips below the uniform flow value. Such a result could be expected because in the recession stage of a flood, the same stage yields lower discharge due to the nature of the water surface elevation along the channel. Maximum dip below the uniform flow value is about 6 per cent of the initial increase in discharge, with the effect vanising with distance. The relative damping is less and speed of the peak is more for higher wave amplitudes. A comparison of Figs. 1 and 2 shows that the nonlinearity effects of Y_w are more pronounced on stage hydrographs than on discharge hydrographs and this is a significant result in the application of unit hydrograph theory.

3.2. *Modification of wave front*

The wave fronts at $T = 3{\cdot}0$ and $6{\cdot}0$ for different wave amplitudes are presented in Fig. 3. Even though the wave starts at the same time for all Y_w cases, it spreads over a larger distance for higher Y_w cases because of its higher speed.

3.3. *Speed of travel of wave peak*

Figure 4 gives the time at which the peak occurs at a particular section for different Y_w values. Wave amplitude has a significant effect on the speed of movement of the

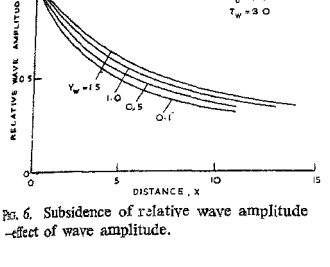

FIG. 6. Subsidence of relative wave amplitude —effect of wave amplitude.

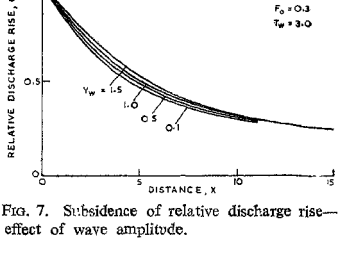

FIG. 7. Subsidence of relative discharge rise— effect of wave amplitude.

wave peak. The wave with higher amplitude moves faster because the celerity of a gravity wave is directly proportional to the square root of depth. If we consider the average speed of travel up to $X = 5$, the wave peak for $Y_w = 1{\cdot}5$ moves 1·46 times faster than for $Y_w = 0{\cdot}1$. As the nondimensional wave speed has been found to be practically independent of F_o and T_w, Fig. 4 can also be used to estimate in a wide channel, the time at which the wave peak would occur at a particular section for any wave amplitude Y_w between 0·1 and 1·5.

The path of the peak of the wave, the path along which depth is 1 per cent above the normal depth and the path of the initial characteristic are presented in Fig. 5 for $Y_w = 0{\cdot}1$ and 1·5. The line along which the depth is 1 per cent above the normal depth moves closer to the initial characteristic for higher Y_w value. It must be noted that 1 per cent rise above the normal depth represents a smaller fraction of the wave amplitude for $Y_w = 1{\cdot}5$ than for $Y_w = 0{\cdot}1$.

3.4. *Subsidence of wave amplitude*

3.4.1. *Subsidence of stage*

Variation of relative wave amplitude Y_w^* with X for different Y_w values is shown in Fig. 6. Y_w^* is defined by

$$Y_w^* = \frac{Y_{max}(X) - 1}{Y_w} \tag{11}$$

Wave amplitude has some effect on the relative damping rate confirming the non-linearity of the phenomenon. The relatively lesser damping for higher wave amplitudes might be partly associated with lesser resistance effects at higher flow depths. The relative wave amplitude Y_w^* is found to vary exponentially with distance X, but the exponent is not a constant for the whole channel reach in contrast to the claim made by Mozayeny and Song[2].

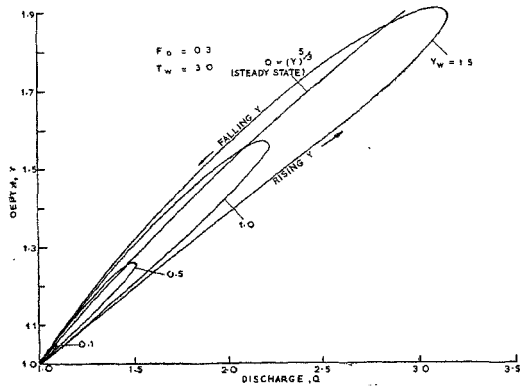

FIG 8 Rating curves for different wave amplitudes

3.4.2. *Subsidence of discharge*

Relative discharge rise Q_w^* is defined as,

$$Q_w^* = \frac{Q_{\max}(X) - 1}{Q_{\max}(O) - 1}. \tag{12}$$

It is seen that at large distances, the effect of Y_w on the relative damping rate is not particularly significant (Fig. 7). In fact, the nonlinearity in the discharge peak is clearly lesser than that in the stage peak as already indicated.

3.5. *Rating curve from computational results*

Figure 8 presents the rating curve for different wave amplitudes as obtained from the computational results at $X = 5$. Greater the wave amplitude greater the difference between the rising and falling stage flood and the results show that there can be very significant difference between the two values. The steady state curve lies between the rising and falling stage values but is closer to the falling stage.

4. Effect of wave duration

4.1. *Modification of hydrographs*

4.1.1. *Stage hydrograph*

Results of hydrographs for different T_w values for $Y_w = 0{\cdot}5$ and $F_o = 0{\cdot}3$ are presented in Fig. 9. In order to facilitate a comparison of the hydrographs for different wave durations the time T is normalised with respect to the wave period T_w by defining

$$T_N = \frac{T}{T_w}. \tag{13}$$

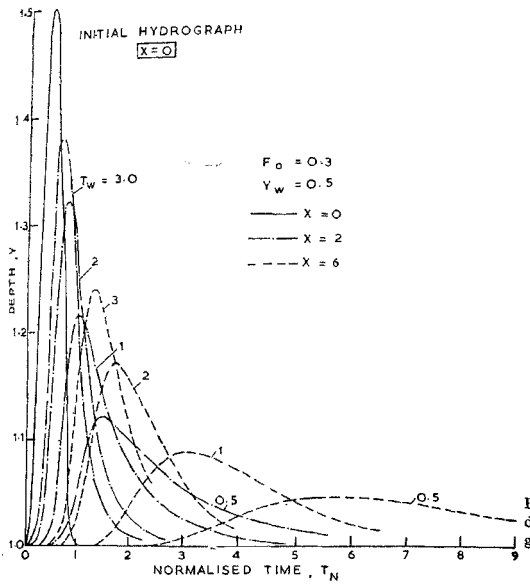

FIG. 9. Effect of wave duration on stage hydrograph.

This makes the initial hydrograph at $X = 0$ common for all T_w values. It is seen from Fig. 9 that the rate of subsidence is very significantly affected by T_w value and the wave with smaller T_w values subsides rapidly. In conjunction with the previous discussion, we see that as the bulk of the wave form reduces, either through reduction of Y_w or T_w, the subsidence rate increases. But a variation in T_w has a much stronger influence than a variation in Y_w.

Larger spread of the wave for lower T_w values is only a scale effect arising from the normalisation of time co-ordinate. The hydrograph for larger T_w values spreads over a larger base time corresponding to the larger base time of the initial hydrograph. Figure 9 clearly shows that the relative rate of spread of the base of the hydrograph is more for smaller T_w values. Hydrograph starts late for lower T_w cases. This is only a scale effect as the speed of the initial disturbance is independent of wave period.

4.1.2. *Discharge hydrograph*

Effect of wave duration T_w on discharge hydrograph is given in Fig. 10. Again the time scale is normalised (eqn. 13) to enable a comparison. There is a significant

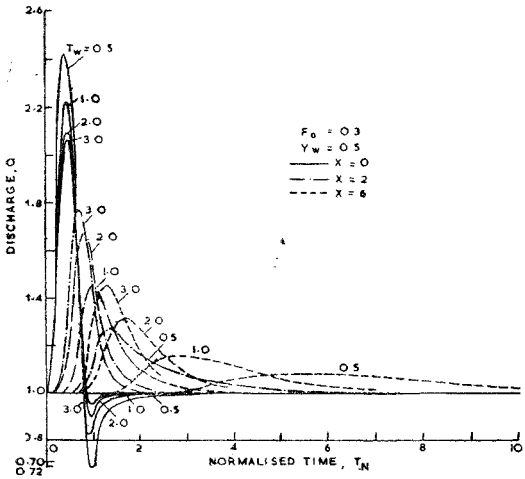

FIG. 10. Effect of wave duration on discharge hydrograph.

variation in the peak of the hydrograph at $X=0$ for different T_w values. The discharge peak is maximum for lowest T_w value. This might be due to the more rapid change in depth corresponding to smaller T_w values. However, the hydrographs at $X = 2$ and 6 show that the peak for smaller T_w values are clearly smaller. This corresponds to the much greater subsidence rate for smaller T_w values as already observed with respect to stage hydrographs (Fig. 9).

4.2. *Modification of wave front*

Figure 11 gives a superimposed picture of the wave front for different wave durations. Wave fronts at $T = 3T_w$ are presented. Thus the instantaneous wave profiles at $T = 1{\cdot}5$, $3{\cdot}0$ and $6{\cdot}0$ are presented for $T_w = 0{\cdot}5$, $1{\cdot}0$ and $2{\cdot}0$ respectively. It is seen from the figure that the wave peak has subsided to a greater extent at $T = 1{\cdot}5$ for $T_w = 0{\cdot}5$ case than at $T = 6{\cdot}0$ for $T_w = 2{\cdot}0$ case. Wave fronts for higher T_w cases have moved a larger distance because of the greater absolute time that has elapsed.

4.3. *Speed of travel of wave peak*

Figure 12 gives the time of arrival of the wave peak at any location. All the computational results for different wave durations lie practically on a single curve indicating that the speed of the wave peak is practically independent of the wave duration. Strictly

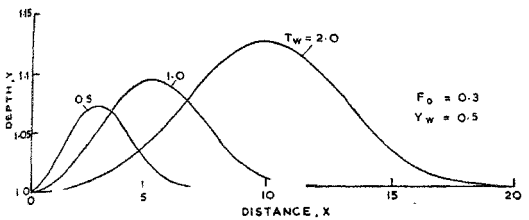

FIG. 11. Effect of wave duration on wave front ($T = 3T_N$).

the speed is seen to be slightly larger for higher T_w values (corresponding to lesser subsidence), but the differences are not significant. It might be noted that Y_w had a fairly significant influence on the wave speed (Fig. 4) in view of larger variation in the flow depth.

4.4. *Subsidence of wave amplitude*

4.4.1. *Subsidence of stage*

Figure 13 presents the variation of relative wave amplitude with distance for different wave durations. The pronounced effect of T_w is clearly brought out by this figure. The rate of subsidence is very high in the initial reaches for low T_w values and the subsidence rate comes down only after the base of the hydrograph has spread significantly at a sufficiently downstream location increasing the local wave duration. Thus we might conclude that a step like flood of small duration existing in isolation subsides rapidly.

4.4.2. *Subsidence of discharge*

Rapid subsidence of the relative discharge rise for low wave durations is clearly seen in Fig. 14. These results also confirm the significant influence of T_w as revealed by Fig. 13.

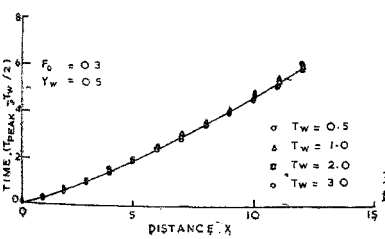

FIG. 12. Speed of travel of wave peak for different wave durations.

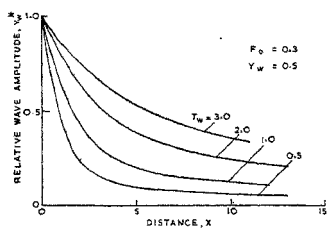

FIG. 13. Subsidence of relative wave amplitude—effect of wave duration.

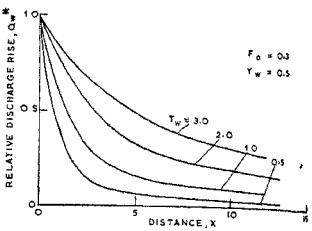

FIG. 14. Subsidence of relative discharge rise—effect of wave duration

4.5. *Rating curve from computational results*

Figure 15 presents the rating curve at $X = 5$ for different wave durations as obtained from computational results. As in the earlier case larger waves yield greater difference between the rising and falling stages and further the steady state curve lies between the rising and falling limbs being closer to the falling limb of the rating curve.

5. Conclusions

Studies are made on the effect of wave parameters (wave amplitude and wave duration) on the propagation of a sinusoidal flood wave in a prismatic wide open channel in which the initial flow is uniform. Aspects studied include modifications of stage hydrographs, discharge hydrographs, wave fronts, speed of travel of the wave peak, subsidence of relative wave amplitude and relative discharge rise and generation of rating curves.

Initial wave amplitude Y_w has some influence on subsidence with lower Y_w values giving slightly higher subsidence. This nonlinearity is found to be slightly lesser in discharge results. Speed of travel of the wave peak is significantly affected by the change in Y_w value with higher Y_w values moving faster.

Wave duration T_w has a pronounced effect on subsidence with subsidence being significantly more for lower T_w values. Further, the rate of subsidence in the initial reaches is very high for lower T_w values suggesting that a step like flood of small duration existing in isolation subsides rapidly. While a moderate variation in T_w affects the rate of subsidence very significantly, it has only a small influence on the speed of the wave peak, with the speed being slightly larger for higher T_w values corresponding to lesser subsidence.

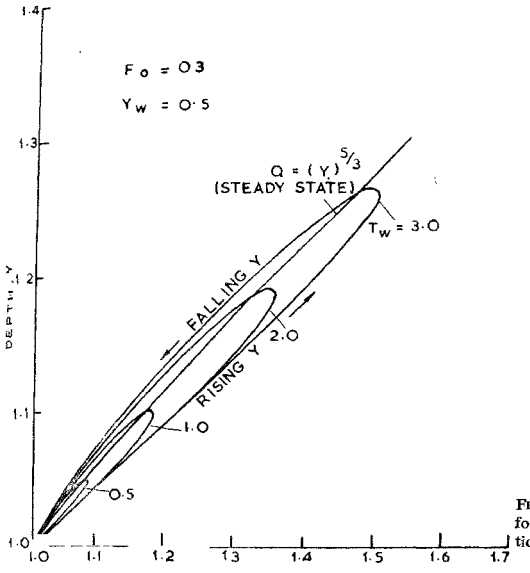

FIG. 15. Rating curves for different wave durations.

References

1. MOHAN KUMAR, M. S. AND SRIDHARAN, K. — Numerical solution of unsteady flows, *Diamond Jubilee Symposium, Central Water and Power Research Station, Poona, India*, Dec. 1976.

2. MOZAYENY, B. AND SONG, C. S. — Propagation of flood waves in open channels, *ASCE Proceedings, J. Hyd. Div.*, 1969, **95**, 877–892.

3. CHIN-LIEN YEN — Subsidence of peak flows in channels, *JAHR, J. Hyd. Res.*, 1978, **16** (4), 309–325.

4. ISAACSON, E., STOKER, J. J. AND TROESCH, B. A. — Numerical solution of flow problems in rivers, *ASCE Proceedings, J. Hyd. Div.*, 1958, **84**, Paper No. 1810.

J. Indian Inst. Sci. 62 (A), Mar 1980, Pp. 71–81

A computational algorithm for the verification of tautologies in propositional calculus

S. V. RANGASWAMY*, N. CHAKRAPANI* AND V. G. TIKEKAR**
Indian Institute of Science, Bangalore 560 012, India.

Received on March 7, 1980.

Abstract

A computational algorithm (based on Smullyan's analytic tableau method) that verifies whether a given well-formed formula in propositional calculus is a tautology or not has been implemented on a DEC System 10. The stepwise refinement approach of program development used for this implementation forms the subject matter of this paper. The top-down design has resulted in a modular and reliable program package. This computational algorithm compares favourably with the algorithm based on the well-known resolution principle used in theorem provers.

Key words : Tautology, propositional calculus, analytic tableau, top-down design, stepwise refinement, Pascal.

1. Introduction

A proof procedure, due to Smullyan[1], that tests whether a given well-formed formula (wff) in Propositional Calculus (PC) is a tautology is known as the analytic tableau method. This paper presents the design and implementation details of a computational algorithm based on the analytic tableau method. The program is developed using the top-down stepwise refinement technique[2, 3, 4] and is coded in Pascal[5]. The program is implemented on a DEC System 10. It comprises 15 procedures and has about 600 lines of Pascal code with a memory requirement of 5K words. The readability and modularity of the program have been greatly enhanced due to the structured programming approach followed in its design.

* School of Automation
** Department of Applied Mathematics

2. Tableau method

The analytic tableau method, a variant of the semantic tableau method of Beth[1], is an elegant and efficient proof procedure for PC. The analytic tableau for a given wff is an ordered dyadic tree, whose root is the negation of the given wff which is to be tested for its validity. For explaining the method of generation of the tableau for a wff requires the notions of subformulas, conjugates,and signed formulas. We briefly present the definitions of these notions in the sequel.

2.1. *Definitions*

(*a*) *well-formed formula (wff)*

A wff in PC is defined recursively as follows :

(i) A propositional variable is a wff, also referred to as an atomic wff.

(ii) If A is a wff, so is $\sim A$.

(iii) If A, B are wffs, so is (AbB), where b is a binary connective.

(*b*) *immediate subformula*

(i) Atomic formulas have no immediate subformulas.

(ii) $\sim X$ has X as an immediate subformula and no others.

(iii) XbY, where b is a binary connective, has X, and Y as immediate subformulas and no others.

(*c*) *subformula*

Y is a subformula of Z if and only if there exists a finite sequence starting with Z and ending with Y such that each term of the sequence except the first is an immediate subformula of the preceding term.

(*d*) *signed formula*

A signed formula is an expression TX or FX, where X is a formula. We normally read TX as 'X is true' and FX as 'X is false'.

(*e*) *conjugate*

The conjugate of a signed formula is the formula obtained by changing the sign. Thus the conjugate of TX is FX, and the conjugate of FX is TX.

2.2. *Analytic tableau*

An analytic tableau for a wff X is an ordered dyadic tree, whose nodes are formulas and whose root is X. The tableau is generated using one of the following four pairs of

rules :

1 (i) If $\sim X$ is true, then X is false.

(ii) If $\sim X$ is false, then X is true.

2 (i) If $X \wedge Y$ is true, then both X and Y are true.

(ii) If $X \wedge Y$ is false, then either X is false or Y is false.

3 (i) If $X \vee Y$ is true, then either X is true or Y is true.

(ii) If $X \vee Y$ is false, then both X and Y are false.

4 (i) If $X \Rightarrow Y$ is true, then either X is false or Y is true.

(ii) If $X \Rightarrow Y$ is false, then simultaneously X is true and Y is false.

The above mentioned rules may be represented in signed formula notation as follows :

1. (i) $\dfrac{T \sim X}{FX}$ (ii) $\dfrac{F \sim X}{TX}$

2. (i) $\dfrac{TX \wedge Y}{\begin{array}{l} TX \\ TY \end{array}}$ (ii) $\dfrac{FX \wedge Y}{FX \mid FY}$

3. (i) $\dfrac{TX \vee Y}{TX \mid TY}$ (ii) $\dfrac{FX \vee Y}{\begin{array}{l} FX \\ FY \end{array}}$

4. (i) $\dfrac{TX \Rightarrow Y}{FX \mid TY}$ (ii) $\dfrac{FX \Rightarrow Y}{\begin{array}{l} TX \\ FY \end{array}}$.

If at any point in the tableau, a formula of the form given in the numerator of any rule appears, then the tableau can be extended on that particular branch by the formula(s) shown in the denominator. In case the denominator contains the '|' symbol, then it is an indication of the fact that the tableau has a branch at that point. The tableau is extended by repeated applications of the rules until no more extensions are possible. A branch of a tableau is closed if and only if it contains some signed formula and its conjugate. The tableau is said to be closed if and only if every branch in it is closed. A proof of an unsigned wff X in the system corresponds to showing that there exists a closed tableau for FX.

The method of proof employing the analytic tableau is shown to be both consistent and complete by Smullyan[1]. The system is consistent since any formula provable by the tableau method is a tautology and the root of any closed tableau is unsatisfiable. The system is complete since for every tautology X there exists a closed tableau with root FX.

3. Program implementation

The program is developed using the top-down stepwise refinement technique[2-4]. The program logic and the various data structures used in these procedures are presented in the sequel*. The problem statement is identified as step 1.

Step 1

Develop a program in Pascal to test whether a given wff in PC is a tautology, using the analytic tableau method.

A given formula has to be tested for its well-formedness, before we can verify whether it is a tautology or not; it may contain operators other than *and, or, not,* and *implies* and hence we need to rewrite the formula into an equivalent form containing only these four operators. These two requirements suggest the step 2 as a refinement of step 1.

Step 2

begin

2.1 Preprocess the input to enable further processing

2.2 Analyse the given wff using the tableau method to verify its validity.

end

The method of analytic tableau successively splits a given formula into its subformulas in an effort to come up with a contradiction. At every stage of computation, it becomes necessary to locate the primary operator in the formula in order to split the given formula into its constituent subformulas. For ease and elegance of computation, the well-known postfix Polish notation is better suited than the conventional infix notation.[9] This consideration along with the need to check the well-formedness of the formula corresponds to the actions in step 2.1. Step 3 presents these details as a refinement of step 2.

Step 3

begin

3.1 Accept a formula from input device.

3.2 *If* operators other than *and, or, not,* and *implies* appear in input *then* reduce the formula into an equivalent formula containing only these four operators.

3.3 convert the formula into postfix Polish notation and check for the well-formedness of input.

* The notation used in stepwise refinement utilizes Pascal-like constructs for depicting control flow.

3.4 Generate the tableau with the negation of the given formula at its root;
if all branches close
then given input wff is a tautology
else given input wff is not a tautology;

end

The steps 3.1 through 3.4 correspond to the preprocessing step and the specifications for these steps are complete. Each of these steps has been coded as a Pascal procedure.

The procedure for input accepts a given wff from a terminal as a string of characters. Every character read from the terminal is appended to a string named ' formula ' in the procedure. The end of input is signalled by a blank character. The input wff is restricted to a maximum length of 80 characters. Any error conditions detected during input are reported to the user.

The input wff in the array ' formula ' is passed on to the procedure that tests whether the given formula contains the *equivalence*, *nand*, or *nor* operators. The computations in this procedure are presented in step 4 which is a refinement of step 3.2†.

Step 4 {refinement of step 3.2}

begin

for every operator in the formula *do*
case operator *of*

$\Leftrightarrow$: rewrite $(\sim \text{opd1} \vee \text{opd2}) \wedge (\sim \text{opd2} \vee \text{opd1})$;
$\uparrow$: rewrite $\sim (\text{opd1} \wedge \text{opd2})$;
$\downarrow$: rewrite $\sim (\text{opd1} \vee \text{opd2})$;
others : skip

end
end

The wff equivalent to the given wff generated in the previous step is processed by the postfix procedure to yield the postfix version of the wff. Conversion to postfix from infix notation is done using the ' shunting yard model ' algorithm due to Dijkstra. This postfix version of the wff is tested to ensure the well-formedness of the given input. The logic of these procedures is presented in step 5.

† The stepwise refinement steps (step 1, step 2, . . .) correspond to completely refined versions. In our presentation, to avoid writing down the same details, in successive steps, we provide only the newly refined section. *E.g.*, step 4 is a refinement of step 3·2; this means that steps 3·1, 3·3 and 3·4 remain unchanged.

```
Step 5 {refinement of step 3.3}
    begin
      for every character in the formula do
        begin if (character = operator)
            then begin
                   while topstack operator priority ≥ current operator priority
                   do push topstack operator to output;
                   push current operator into stack
                   end
            else begin
                   if (character = '(')
                   then increase priority of all operators by the standard value
                   else
                   if (character = ')')
                   then decrease priority of all operators by the standard value
                   else push in ouput area
            end;
            if stack not empty
            then pop contents of stack and push them into output
        end;
        for every character in the formula do
        case character of
            Operands : associate weight – 1;
            Unary operator : associate weight 0;
            Binary operator : associate weight 1
            end;
        if sum of weights = – 1
        then formula is well-formed
        else formula is not well-formed;
    end.
```

This completes the preprocessing of input. Step 3.4 pertains to the processing based on the tableau method. Before we embark on the stepwise refinement of this step further, we need to decide about the data structures and control flow organization. The tableau is an ordered dyadic tree and a path in the tree consists of an ordered set of formulas. The method requires the testing of every path to find out whether it is closed and hence there is no need to maintain the complete tableau in the memory. For reasons of efficient core utilisation, only one path of the tableau is maintained at a time in the memory. An array is used to hold all the formulas in a path in contiguous locations as the processing on these formulas is strictly sequential. An array of pointers to this 'formula array' is maintained to identify the beginning of every formula in this data structure. To enable the generation of a path in the tableau in a systematic fashion, an array indicating the parent formula of a given sub-

formula is also maintained. The rules defining the construction of the tableau are coded as individual procedures. The main procedure is recursively invoked to enable the complete generation of a path. Once a path is completely constructed, another procedure scans all the signed atomic formulas to determine whether the path is closed. The main procedure provides the necessary pointers to access atomic formulas in the array, thereby avoiding searches to locate them. If a path is closed, the main procedure tests whether there are any unexplored paths in the tableau and if so, proceeds with the next path. A stack of branch pointers is maintained so that the various paths in the tableau are scanned in a left-to-right manner. If any open path (a path that is not closed) is detected, the processing is terminated with a message that the given formula is not a tautology. If all the paths are closed in the tableau, then the program declares that the given formula is a tautology. With the above mentioned control strategy and data structure organization as the base, we present below the refinement of step 3.4 in steps 7 and 8.

```
Step 7
   begin prefix an F to the wff in postfix notation.
    repeat
      repeat
        for every formula do
          case primary operator of
            not : change sign of formula;
            and : separate left operand (lhs) and right operand (rhs); 'andprocess';
            or : separate lhs and rhs; 'orprocess';
            implies : separate lhs and rhs; 'implyprocess'
          end;

      until path is complete;
      collect all atomic formulas in the path;
      if both TX and FX exist in this collection
      then declare path closed
      else declare path is open and set flag;
    until nomorepaths or flagset;
          if noflagset
          then declare given wff is a tautology
  end

Step 8 {refinement of 'andprocess'}
   begin
     if sign is T
       then extend current path with two subformulas T(lhs) and T(rhs)
       else begin
            set a flag to indicate branch at that point and stack the pointer;
            if first traversal then extend current path with F(lhs)
```

```
                    else begin
                          extend current path with F(rhs);
                          pop up branch stack
                         end
            end
    end
```

The refinements of steps ' orprocess ' and ' implyprocess ' are similar to step 8.

4. Illustrative examples

We provide below sample outputs generated by the program for two specific inputs. Every path is listed starting from the origin, for easy perusal; the actual implementation does not generate every branch from the origin. The first input wff is a tautology and the second input wff is not a tautology†.

EXAMPLE 1

input : (PA (QKR)) C ((PAQ)K(PAR))

output :

```
GIVEN FORMULA IS WELL-FORMED
    FPQRKAPQAPRAKC
    FPQAPRAK
    TPQRKA
    FPQA
    TP
    FP
    FQ

BRANCH CLOSED
    FPQRKAPQAPRAKC
    FPQAPRAK
    TPQRKA
    FPQA
    TQRK
    FQ
    FP
    TQ
    TR
```

† For purposes of computer implementation A, K, N, C are used to represent the operators *or*, *and*, *not*, and *implication* respectively.

```
BRANCH CLOSED
   FPQRKAPQAPRAKC
   FPQAPRAK
   TPQRKA
   FPRA
   TP
   FP
   FR

BRANCH CLOSED
   FPQRKAPQAPRAKC
   FPQAPRAK
   TPQRKA
   FPRA
   TQRK
   FP
   FR
   TQ
   TR

BRANCH CLOSED
GIVEN FORMULA IS A TAUTOLOGY
EXAMPLE 2
input :  (PAQ)C(PKQ)
output :
GIVEN FORMULA IS WELL-FORMED
   FPQAPQKC
   FPQK
   TPQA
   FP
   TP
BRANCH CLOSED
   FPQAPQKC
   FPQK
   TPQA
   FP
   TQ
BRANCH OPEN
HENCE NOT A TAUTOLOGY
```

5. Remarks and conclusions

This computational algorithm has not so far been used in theorem-provers; most of the well-known implementations of theorem-provers make use of the resolution

principle[7]. The resolution-based systems basically require that the wff be presented in clause form; normally a wff is not available in clause form and the task of converting a wff into clause form is by itself of exponential complexity. The analytic tableau method does not have any such special input requirements.

The resolution method requires that the empty clause be generated from the given clauses by successively resolving them. As there is no algorithmic way to decide which of the given clauses yield the empty clause by resolving, refinements to resolution by means of heuristics aim at reducing the searches through blind alleys. In contrast, the analytic tableau method, essentially breaks a formula into its constituents (subformulas); the process is a systematic one and terminates much faster compared to the resolution technique.

The method of Davis and Putnam[8] is another method used in one of the efficient automatic theorem-provers. This method is based on the four rules—tautology rule, one-literal rule, pure literal rule and splitting rule. This method also requires that the given formula be in conjunctive normal form so that any of the four rules may be applied. In the method of analytic tableau there is no need for a given wff to be in conjunctive normal form. Also at each step of the generation of the tableau, the principal connective of the signed formula of a node enables the determination as to which of the eight rules is to be applied; in the method of Davis and Putnam an analogous determination as to which of the four rules is to be applied is not possible.

The implementation of the tableau method ensures that the number of branches of the generated tableau is minimum by judiciously ordering the subformulas generated at each step. The depth-first approach of generating each path in the tableau, in the left-to-right order, results in reduced main storage requirements for the program. Each rule of this method has been coded as a procedure resulting in a neatly structured program enhancing its readability and modularity.

6. Acknowledgements

We express our gratitude to Professor R. Narasimhan, Director, National Centre for Software Development and Computing Techniques, Bombay, for providing the necessary computational facilities to enable this implementation.

References

1. Smullyan, R. M. *First-order logic*, Springer-Verlag, 1968.

2. Wirth, N. Program development by stepwise refinement, *CACM*, **14**, 4, 1971, 221–227.

3. Dijkstra, E. W. Notes on structured programming, in *Structred programming* by Dahl, Dijkstra, and Hoare, Academic Press, 1972.

4. KIEBURTZ, R. B. *Structured programming and problem solving with Algol–W*, Prentice-Hall, 1975.

5. JENSEN, K. AND WIRTH, N. Pascal : User Manual and Report, *Lecture Notes in CS*, **18**, Springer-Verlag, 1974.

6. BETH, E. W. *The foundations of mathematics*, North Holland, 1959.

7. ROBINSON, J. A. A machine-oriented logic based on the resolution principle, *JACM*, **12**, **1**, 23–41.

8. DAVIS, M. AND PUTNAM, H. A computing procedure for quantification theory, *JACM*, **7**, 1960, 201–215.

J. Indian Inst. Sci. 62 (A), Mar 1980, Pp. 83–88

Nonlinear I–V characteristics of semiconducting paints

D. B. GHARE AND C. R. VARADARAJ*
Department of High Voltage Engineering, Indian Institute of Science, Bangalore 560 012.

Received on November 13, 1979; Revised on March 8, 1980.

Abstract

Tin oxide-based high resistivity semiconducting paints can be used on high voltage insulators for improved performance. They were found to exhibit nonlinear I–V characteristics which are reported here. The paints exhibited power law relationship and a sharp transition in mechanism of conduction at a critical voltage.

Key words: Conducting paints, electrical properties.

1. Introduction

Semiconducting glazes are employed on high voltage insulators for improving their performance in several respects[1–4] such as reduction in radio interference (R.I.) and corona, suspension of pollution flash over (F.O.), uniform voltage distribution, prevention of condensation of fog, moisture and ice, etc.

Recently semiconducting paints have also been reported to be useful in suppression of R.I. and corona and pollution F.O. under laboratory as well as severe outdoor conditions[5–6]. Some of their interesting properties have been reported earlier[7]. During further work on development of such paints they were found to exhibit interesting nonlinear I–V characteristics which are reported here.

2. Experimental

Three varieties of semiconducting paints were prepared by using antimony-doped semiconducting tin oxide as the basic semiconducting material and three types of oil media, *viz.*, linseed oil, karanja oil and cottonseed oil. The semiconducting tin oxide

* Tata Consulting Engineers, Bombay.

was prepared by doping the material with antimony oxide at 1200 ± 10° C for 5 hr. The fine powder (– 150 mesh) of this doped semiconducting tin oxide was then intimately mixed with the above oil media, to obtain three varieties of semiconducting paints.

Silver paste contacts were painted on glass specimens and fired at 600° C for 30 min to achieve good adhesion. Electrical contact leads were then soldered on to the fired silver contacts. The desired semiconducting paint was then spray painted on these specimens and these specimens were then cured in an electrical oven at 105° C for 500 hr to stabilise the electrical resistivity of these samples. The I–V characteristics of such cured paint samples were then measured using ac voltages in the range 100-1500 V. The details regarding the specimens and the circuit diagram used for the measurement of I–V characteristics are shown in Fig. 1.

The resistance of the paint samples was found to be a function of applied voltage. The resistance values at various applied voltages were therefore inferred from the I-V characteristics.

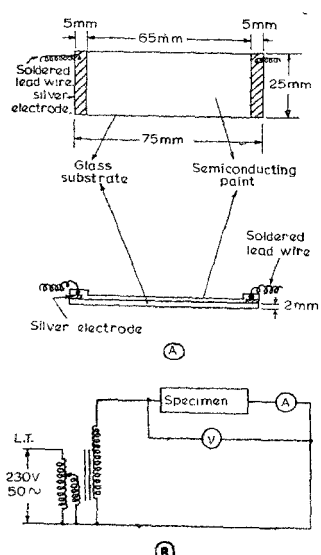

FIG. 1. (A) Details of specimen painted with semiconducting paint. (B) Circuit diagram for the measurement of I–V characteristics.

3. Results and discussion

From the typical I–V characteristics exhibited by the paints, shown in Fig. 2, it can be seen that these paints do not exhibit linear ohmic I–V characteristics. The typical resistance *vs.* voltage characteristics of such paints are shown in Fig. 3. From this figure it can be seen that the resistance of the paints initially increases with increase in the applied voltage and attains a maximum at a critical applied voltage. Above this critical voltage, the resistance starts decreasing with further increase in the applied voltage.

Some typical log-log plots for the I–V characteristics of these paints are shown in Fig. 4. It can be seen from this figure that the log-log plots of I–V characteristics of such paints are linear which indicates that the paints exhibit power law relationship of the type

$$V = K \cdot I^{\beta} \tag{1}$$

where

V = applied voltage

I = current

K = a constant depending on composition and dimensional properties

β = the exponent—constant indicating the extent of nonlinearity in I–V characteristics.

Further, it can be seen from Fig. 4 that the paints exhibit same relationship below and above a critical voltage, but the slope of the line changes at the critical voltage. This indicates that the values of the constants K and β are abruptly changing at the critical voltage. This indicates that there is a transition in the mechanism of conduction at the critical voltage V_c. The values of the exponent β below and above V_c for various paint samples are given in Table I. It can be seen from this table that the

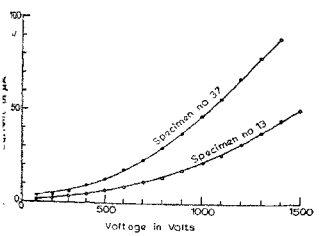

G. 2. The typical I–V characteristics of tin ide-based semiconducting paints.

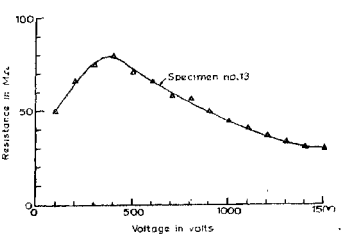

FIG. 3. Typical resistance—voltageche aracteristics of the tin oxide-based semiconducting paints.

values of β are more than unity for voltages below V_c and less than unity for voltages above V_c. The mechanism of conduction above V_c therefore seems to resemble the mechanism of conduction observed in SiC voltage dependent resistors[8-11]. The mechanism of conduction at low fields below V_c may be controlled by the diffusion of charge carriers through the nonconducting medium. The values of β below and above V_c seem to be dependent on the nature of the nonconducting organic medium.

The mechanism of electrical conduction in silicon carbide voltage dependent resistors has been explained on the basis of two types of hypothesis. In the first case, it is proposed that every *p*-type grain of SiC has a coating of a thin layer of *n*-type material. The sintered polycrystalline compacts therefore act like a large number of *p–n* junction diodes connected in series and parallel in random directions. Two *p–n* junction diodes connected in parallel but in reverse direction would indeed give a symmetric nonlinear behaviour. The SiC VDRs, it is suggested, are a result of a number of such pairs of diodes connected in series and parallel to each other. This theory obviously cannot explain the mechanism of conduction in the semiconducting paints, because sintered products of *n*-type SnO_2 do not show this type of behaviour and hence the formation of *p–n* junctions has to be ruled out. Another mechanism suggested is based on the fact that each SiC grain has a thin protective layer of SiO_2 on its surface. This layer protects it from further oxidation and is responsible for the high temperature withstand capability of the SiC products. In case of sintered VDRs, this protective layer acts as an insulating barrier and electrons have to tunnel through this barrier in order to reach the bulk of the adjacent grain. This tunnelling across the SiO_2 insulating barrier at the surface of each grain is suggested to be responsible for the nonlinear

Table I

Typical values of the exponent β for various compositions

Sl. No.	Composition in gm/litre	Organic medium	Value of β	
			below V_c	above V_c
1.	710	Linseed oil	1·724	0·7042
2.	1000	Linseed oil	1·429	0·6757
3.	1600	Linseed oil	1·538	0·6757
4.	710	Karanja oil	1·600	0·5495
5.	1000	Cotton seed oil	1·379	0·4926

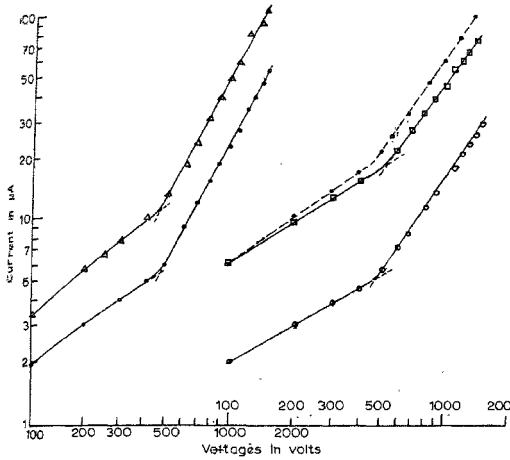

FIG. 4. Typical I–V characteristics on log-log scale.

behaviour of the SiC voltage dependent resistors. It is possible to explain the nonlinear behaviour of the semiconducting paints on the basis of this model. The thin dielectric insulating layer, provided by the organic medium, coats the surface of the semiconducting tin oxide grains. The electrons therefore have to overcome this insulating barrier in order to be able to reach the bulk of the adjacent tin oxide grains.

4. Conclusion

The semiconducting paints based on the oxide as the basic semiconducting material exhibit nonlinear I–V characteristics and follow the power law relationship.

The mechanism of conduction in such paints exhibits a sharp transition at a critical voltage V_c and the mechanism of conduction above V_c seems to be similar to that exhibited by silicon carbide nonlinear voltage dependent resistors.

The nonlinearity as indicated by the value of the exponent 'β' is dependent on the nature of the organic insulating medium.

5. Acknowledgement

The authors thank Professor G. R. Govinda Raju for his kind encouragement and support.

References

1. CLARK, C. H. W. — Semiconducting glaze on high voltage insulators, *Elect. Rev.* 1964 **174**, 740.
2. MORAN, J. H. AND POWELL, D. G. — *Trans. IEEE, Power Apparatus and Systems*, 1972, *PAS*-**91**, 2452-2457.
3. GHARE, D. B. — *Semiconducting glazes for high voltage insulators*, Indo-Soviet Conference on Solid State Materials, Bangalore, 1972, Session E, Paper No. 14.
4. FUJIMURA, T., NAITO, K. AND IRIC, T. — *Trans. IEEE, Power Apparatus and Systems*, 1978, *PAS*-**97**, 763-771.
5. PARTHASARATHY, G. AND GHARE, D. B. — *Reduction in radio noise level of high voltage insulators by the application of semiconducting paint*, National Seminar on Electrical Insulation, Institution of Engineers, Bangalore, 1974, Session III, Paper No. 6.
6. SRIKANTAN, D. L. AND GHARE, D. B. — *Pollution hazards faced on 220 kV electromagnetic potential transformers at Tarapur atomic power station switchyard and the improvements resulting from the application of the semiconducting paint*, Central Board of Irrigation and Power, 45th Annual Research Session, Hyderabad, 1976, **4**, 119–121.
7. GHARE, D. B. — Tin oxide based semiconducting paints and their electrical properties, *Indian J. Technol.*, 1977, **15**, 67–70.
8. SCHWERTZ, F. A. AND MAZENKO, J. J. — Nonlinear semiconductor resistors, *J. Appl. Phys.*, 1953, **24**, 1015–1024.
9. GOFFAUX, R. — Electrical properties of silicon carbide varistors, *Proceedings of the conference on silicon carbide, A high temperature semiconductor.* April 1959, Boston, Pergamon Press, 1960, pp. 462–481.
10. IVANOV, L. I. AND PRUZHININA GRANOVSKAYA, V. I. — *Soviet Phy. Tech. Phy.*, 1956, **1**, 216–227.
11. JACQUES SUCHET — Nonlinear electric resistors, *U.S. Patent* 2, **714**, **096**, 26 July 1955.